

## Phase Separation in the Itinerant Metamagnetic Transition of $\text{Sr}_4\text{Ru}_3\text{O}_{10}$

Z. Q. Mao,<sup>1,\*</sup> M. Zhou,<sup>1</sup> J. Hooper,<sup>1</sup> V. Golub,<sup>2</sup> and C. J. O'Connor<sup>2</sup>

<sup>1</sup>Department of Physics, Tulane University, New Orleans, Louisiana 70118, USA

<sup>2</sup>Advanced Materials Research Institute, University of New Orleans, New Orleans, Louisiana 70148, USA

(Received 2 May 2005; published 23 February 2006)

We have investigated the electronic transport properties of the triple-layered ruthenate  $\text{Sr}_4\text{Ru}_3\text{O}_{10}$ . We observed surprising anomalous features near its itinerant metamagnetic transition, including ultrasharp magnetoresistivity steps, a nonmetallic temperature dependence in resistivity for upward field sweeps, and a resistivity drop in temperature dependence for downward field sweeps. These features suggest that the metamagnetic transition of  $\text{Sr}_4\text{Ru}_3\text{O}_{10}$  occurs via an electronic phase separation process with magnetic domain formation.

DOI: 10.1103/PhysRevLett.96.077205

PACS numbers: 75.30.Kz, 71.27.+a, 75.47.-m, 75.60.Ch

Perovskite ruthenates of the Ruddlesden-Popper (RP) series  $\text{Sr}_{n+1}\text{Ru}_n\text{O}_{3n+1}$  show fascinating physics, such as spin-triplet superconductivity in  $\text{Sr}_2\text{RuO}_4$  ( $n = 1$ ) [1–3], and metamagnetic quantum criticality in  $\text{Sr}_3\text{Ru}_2\text{O}_7$  ( $n = 2$ ) [4–7].  $\text{Sr}_4\text{Ru}_3\text{O}_{10}$  is the  $n = 3$  member of the RP series; it is a structurally distorted ferromagnet with a Curie temperature  $T_C = 105$  K and a saturated moment of  $\sim 1.0\mu_B/\text{Ru}^{4+}$ , directed primarily along the  $c$  axis [8,9]. Its ferromagnetic (FM) transition is followed by an additional magnetic transition at  $T_M = 50$  K. The magnetic state below  $T_M$  depends on the field orientation. When the field is applied along the  $c$  axis ( $H \parallel c$ ), the ferromagnetism is enhanced and the magnetic susceptibility shows an additional increase below 50 K; for in-plane fields ( $H \parallel ab$ ) the system switches to an itinerant metamagnetic state and a pronounced peak occurs in susceptibility at 50 K. The metamagnetic transition occurs at about 2 T for  $H \parallel ab$  and exhibits significant hysteresis in the downward field sweep [8,9]. Recent Raman spectra measurements on  $\text{Sr}_4\text{Ru}_3\text{O}_{10}$  [10] suggest that this metamagnetic transition is associated with the canted orientation of the Ru moments. In the temperature range  $T_M < T < T_C$ , the canted Ru moments are ferromagnetically aligned along the  $c$  direction, but have no net in-plane ordering for in-plane fields. However, for  $T < T_M$ , the moments “lock” into a canted antiferromagnetic (AFM) configuration for in-plane fields less than 2 T, and into a canted FM configuration for in-plane fields higher than 2 T [10].

The itinerant metamagnetism of the double-layered  $\text{Sr}_3\text{Ru}_2\text{O}_7$  has recently attracted widespread attention since it shows a metamagnetic quantum critical end point [4–7]. In the vicinity of this point, a new ordered phase with increased resistivity was recently discovered [6]. These exciting features open new routes to explore the novel physics of quantum criticality. Since  $\text{Sr}_4\text{Ru}_3\text{O}_{10}$  is the nearest neighbor to  $\text{Sr}_3\text{Ru}_2\text{O}_7$  in the RP series, further investigation on the itinerant metamagnetism of this material is expected to provide important insight into the nature of metamagnetic quantum criticality in  $\text{Sr}_3\text{Ru}_2\text{O}_7$ .

We have performed systematic measurements of the in-plane electronic transport properties of  $\text{Sr}_4\text{Ru}_3\text{O}_{10}$  for  $H \parallel$

$ab$  using high-quality single crystals. We have observed strong evidence that the metamagnetic transition of  $\text{Sr}_4\text{Ru}_3\text{O}_{10}$  occurs via a phase separation process with magnetic domain formation. Magnetic domains in the context of itinerant metamagnetism have only recently been considered theoretically [11]; to our knowledge, no substantial experimental evidence for their existence has been reported.

Our crystals were grown by a floating-zone (FZ) technique [12]. Crystals selected for the measurements were well characterized by x-ray diffraction and were found to be pure  $\text{Sr}_4\text{Ru}_3\text{O}_{10}$ . The transport data presented in this Letter were obtained on a crystal with a residual resistivity  $\rho_0 = 6.2 \mu\Omega \text{ cm}$ . Our measurements were carried out in a <sup>3</sup>He cryostat using a standard four-probe technique.

Figure 1(a) shows the magnetization as a function of magnetic field at 2 K for a FZ-grown  $\text{Sr}_4\text{Ru}_3\text{O}_{10}$  crystal. Similar to the results obtained on flux-grown crystals [8,9], we observed ferromagnetic behavior for  $H \parallel c$  and a metamagnetic transition accompanied by significant hysteresis at about 2 T for  $H \parallel ab$ . Near the metamagnetic transition, the in-plane resistivity  $\rho_{ab}$  exhibits a sharp change, as shown in Fig. 1(b) where  $B_{c1}$  ( $\sim 1.75$  T) and  $B_{c2}$  ( $\sim 2.50$  T) are defined as the lower and upper critical fields of the transition for an upward sweep of magnetic field. Of particular interest is that  $\rho_{ab}$  displays steps as the field sweeps down through the transition. These steps are extraordinarily sharp, as shown in the main panel of Fig. 1 where the data were taken with a step of 1 G. The characteristics of the steps depend sensitively on the level of disorder; for example, a sample with  $\rho_0 = 8.7 \mu\Omega \text{ cm}$  exhibits only a single step.

Our systematic measurements and analyses suggest that these ultrasharp magnetoresistivity steps originate from an electronic phase separation process with magnetic domain formation. For fields well above the transition, both magnetization and  $\rho_{ab}$  tend to saturate, indicating that the system is close to being fully polarized. We define the system as a forced-ferromagnetic (FFM) state for this field regime. For fields well below the transition, we define the system as being in a lowly polarized (LP) state. Whether

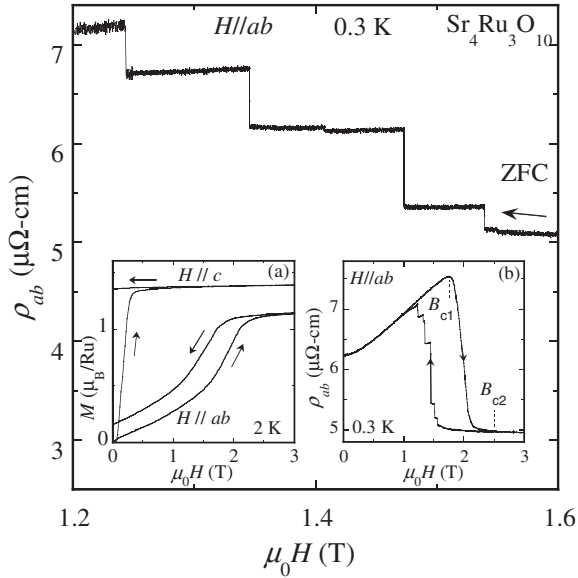


FIG. 1. Downward field sweep of in-plane resistivity  $\rho_{ab}$  for  $H \parallel ab$ . Inset (a) magnetization as a function of magnetic field for both  $H \parallel c$  and  $H \parallel ab$ . Inset (b) field sweeps of  $\rho_{ab}$  within the range 0–3 T for  $H \parallel ab$ .  $B_{c1}$  is defined as the lower critical field of the transition where  $\rho_{ab}$  shows a peak;  $B_{c2}$  is defined as the upper critical field above which  $\rho_{ab}$  tends to saturate.

this LP phase is in an antiferromagnetic canted configuration as suggested by Raman spectra measurements [10] is yet to be verified. Near or within the transition regime, our data demonstrate that the system exists as a LP-FFM mixed phase. Magnetic domains form as the field sweeps through the transition. Since the FFM phase has lower resistivity than the LP phase, the LP-FFM mixed phase process manifests itself through very unique characteristics as stated below.

Figure 2(a) shows the data taken in different field-sweep cycles using zero-field cooling (ZFC). For each cycle, the field first sweeps from zero up to a certain value following the ZFC history, then sweeps back towards zero. We note that  $\rho_{ab}$  decreases nearly linearly in the downward sweep when the maximum field of the sweep is below  $B_{c1}$ , but shows very unusual hysteretic behavior when the maximum field is slightly higher than  $B_{c1}$  [e.g., see the data taken with a maximum field of 1.90 T in Fig. 2(a)].  $\rho_{ab}$  first decreases linearly, then increases prominently after a broad minimum and subsequently shows steps. This behavior can best be understood as resulting from an inhomogeneous phase in which FFM domains are embedded within a LP matrix. The initial linear decrease is due to the LP-phase's dominant contribution to transport, while the prominent increase below the minimum, as well as the significant hysteresis, reflects the FFM-phase's contribution.

As the maximum field of the sweep increases, the volume fraction of the forced-ferromagnetic phase should increase; eventually, as the maximum field approaches  $B_{c2}$ , FFM domains should form a percolative network that dominates transport properties. This conjecture is fully

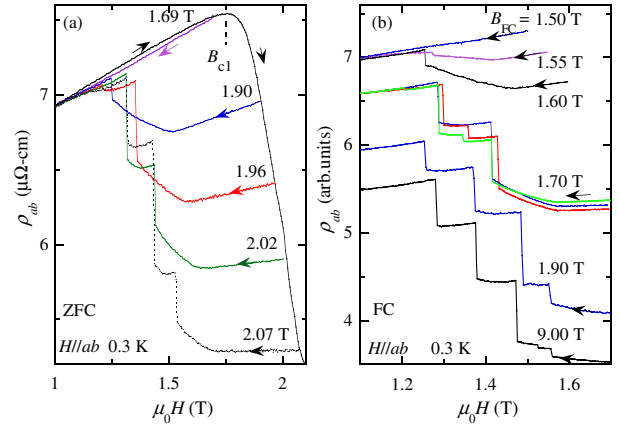


FIG. 2 (color online). Field sweeps of  $\rho_{ab}$  for  $\text{Sr}_4\text{Ru}_3\text{O}_{10}$  under (a) various zero-field cooling (ZFC) and (b) field-cooling (FC) histories. Labels in (a) indicate the upper limit of the field sweep during ZFC measurements.  $B_{\text{FC}}$  in (b) is the field used for field cooling. The data for FC at 1.70, 1.90, and 9.00 T in (b) are shifted for clarity.

consistent with our observation: the slope of the initial linear part of resistivity during a downward sweep (which reflects the LP-phase's contribution to transport) decreases gradually with increasing maximum field and becomes zero as the maximum field approaches  $B_{c2}$  (e.g., see the data taken with the maximum field of 2.07 T). In addition, we find that the characteristics of the steps depend on the maximum field of the sweep; when it is past  $B_{c1}$ , the steps appear and grow in number with increasing maximum field. The origin of these steps can be well understood in this phase separation picture (see below for detailed discussions).

For comparison, we also performed measurements under field cooling (FC), which provides further support for the existence of phase separation. As seen in Fig. 2(b), although the initial field  $B_{\text{FC}}$  for the downward sweep is below the transition,  $\rho_{ab}$  exhibits features of mixed phases similar to those seen in measurements with ZFC; namely, it shows a minimum and steps (see the data taken with  $B_{\text{FC}} = 1.55, 1.60$  and  $1.70$  T). This behavior can be understood as follows: the FC process favors ferromagnetic domains, resulting in an increase in the volume fraction of the FFM phase and leading the system into a mixed state even for fields below  $B_{c1}$ . We made three independent measurements of magnetoresistivity using FC at 1.70 T. Despite identical cooling histories, we observed slight shifts in the positions of the steps, which reflect the non-equilibrium character of the mixed state. Further increasing  $B_{\text{FC}}$  results in a greater number of steps.

Evidence for phase separation was also observed in the temperature dependence of resistivity. Figure 3(a) shows  $\rho_{ab}(T)$  at various fields for an upward field sweep.  $\rho_{ab}$  displays a remarkable nonmetallic temperature dependence within the transition regime, in sharp contrast with the behavior seen outside this region where  $\rho_{ab}$  shows  $T^2$  dependence for  $B < B_{c1}$ , and  $T^{5/3}$  dependence

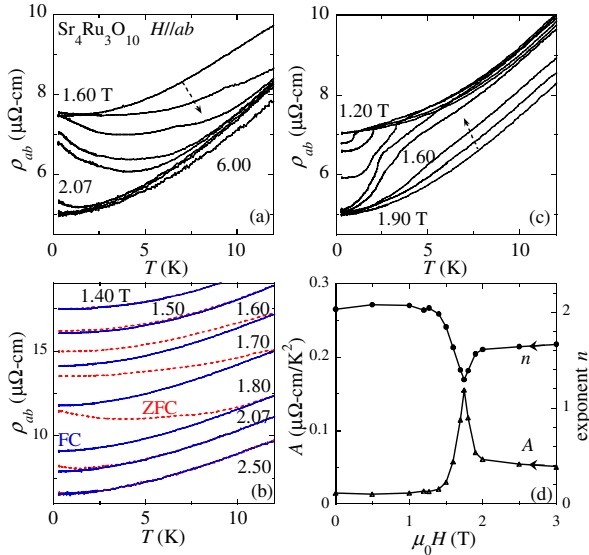


FIG. 3 (color online). (a)  $\rho_{ab}(T)$  at  $\mu_0 H = 1.60, 1.75, 1.82, 1.89, 1.92, 2.07, 2.50, 6.00$  T in the upward sweep of magnetic field. Each curve was measured by warming up after zero-field cooling (ZFC). (b)  $\rho_{ab}(T)$  at various fields for the upward sweep for field cooling (blue solid curves); data for ZFC (red dashed curves) are included for comparison. Data are shifted for clarity. (c)  $\rho_{ab}(T)$  at  $\mu_0 H = 1.20, 1.27, 1.40, 1.50, 1.55, 1.60, 1.70, 1.75, 1.90$  T in the downward field sweep. The data were taken by warming up after first ZFC, then increasing the field up to 3 T to enter the fully polarized state, and subsequently decreasing the field down to the target value. (d) Parameters extracted from fitting the data in the 5–12 K range of Fig. 3(c) to  $\rho = \rho_0 + AT^n$ . The divergence of  $A$  at 1.75 T, as well as the sharp change of  $n$ , indicates that the transport properties near the transition are affected by critical fluctuations.

for  $B > B_{c2}$ . This observation seems surprising, but fits very well into the above picture of phase separation. As indicated above, prominent FFM domains should develop in the transition region  $B_{c1} < B < B_{c2}$ . The nonmetallic behavior in transport within this field range is likely due to scattering off of the boundaries of these FFM domains. This is supported by the observation that a field-cooling process can suppress the nonmetallic behavior, as seen in Fig. 3(b). As mentioned above, the field-cooling process increases the volume fraction of the FFM phase; this would allow metallic percolative transport through the FFM phase at any field within the transition. Moreover, we find that the irreversibility in  $\rho_{ab}(T)$  between ZFC and FC develops starting at 1.4 T, implying that FFM domains start to develop even below the lower critical field  $B_{c1}$ .

We also measured the temperature dependence of  $\rho_{ab}$  at various fields during downward field sweeps. As seen in Fig. 3(c),  $\rho_{ab}(T)$  shows a striking drop within the same field range (1.2–1.6 T) where the field sweep of  $\rho_{ab}$  exhibits ultrasharp steps, in sharp contrast with the nonmetallic temperature dependence seen in the transition range of the upward field sweep. This surprising feature can be interpreted within the picture of a LP-FFM mixed phase as well; the related discussion is given below.

The schematic in Fig. 4 summarizes the mixed phase process through the metamagnetic transition of  $\text{Sr}_4\text{Ru}_3\text{O}_{10}$ . For the upward field sweep, the field starts to induce FFM domains below  $B_{c1}$ ; transport properties, however, are still dominated by the LP phase until the field approaches  $B_{c1}$ . For fields above  $B_{c1}$  but lower than  $B_{c2}$ , FFM domains grow remarkably and domain boundary scattering dominates the transport properties at low temperature [see Fig. 4(a)], resulting in a nonmetallic temperature dependence in  $\rho_{ab}$ . As the field approaches  $B_{c2}$ , FFM domains form a percolative network [see Fig. 4(b)]. For the downward field sweep in the situation with the maximum field of the sweep above  $B_{c2}$ , LP domains develop as the field enters the range 2 T–1.6 T and are embedded in the FFM matrix [see Fig. 4(c)]. Transport properties in this circumstance are dominated by the FFM matrix since the FFM phase has lower resistivity. As the field sweeps down further, below 1.6 T, more LP domains occur and grow bigger, so that they are spontaneously connected and form continuous domain walls at certain threshold fields [see Fig. 4(d)]. These abruptly hinder the current flow in the FFM matrix, resulting in ultrasharp steps in magnetoresistivity.

Since the system is initially in a uniform FFM state for a downward sweep and since the volume ratio of FFM/LP phase is temperature dependent, the resistivity drop at low temperatures observed between 1.6 and 1.2 T [see Fig. 3(c)] can be attributed to an increase of the volume fraction of the FFM phase caused by decreasing temperature, which would restore FFM percolative transport. This point of view is supported by the observation that the decrease of temperature at 1.55 or 1.60 T causes  $\rho_{ab}$  to decrease to the same value as that for high applied fields, where the transport is dominated by a FFM percolation network.

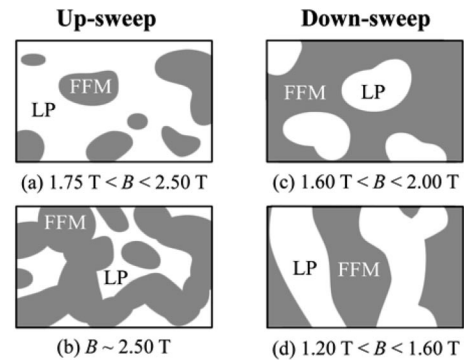


FIG. 4. Schematics of the lowly polarized (LP)–forced-ferromagnetic (FFM) mixed phase process through the metamagnetic transition of  $\text{Sr}_4\text{Ru}_3\text{O}_{10}$  for both the upward field sweep (left column) and the downward field sweep (right column). For the upward sweep, FFM domains do not form a percolative network until the field approaches  $B_{c2}$ ; for the downward sweep, LP domains form continuous walls when the field is below 1.6 T.

The dynamic behavior of the steps under different cooling histories, shown in Fig. 2, can be understood within this picture of mixed phases. The nonequilibrium character of the steps suggests that these domain walls are not static but fluctuating, as would be expected. The volume fraction of the FFM phase will become larger with an increase of the maximum applied field during a zero-field-cooling measurement or an increase in the cooling field  $B_{FC}$  for a field-cooling measurement; this would in turn cause an increase in the number of LP domain walls and the number of steps as the field sweeps down through the transition. One may ask why the steps do not occur during upward field sweeps. This might be attributed to the fact that the initial state before the transition and the dynamic process of magnetic domain formation in the upward field sweep differ from those of the downward field sweep, resulting in different domain boundary scattering for the two situations. One possible scenario is that the change in domain boundary scattering is more continuous in the upward field sweep, but occurs abruptly at certain threshold field values in the downward field sweep. Further investigation is required to fully understand this issue.

Next, we examine what comparisons can be drawn between  $Sr_4Ru_3O_{10}$  and  $Sr_3Ru_2O_7$ . First of all, we would like to point out that metamagnetic transitions should generally change from first order to a crossover above a critical temperature  $T^*$ . Our measurements show that  $T^*$  in  $Sr_4Ru_3O_{10}$  is about 20 K: below this temperature the transition is first order and shows hysteresis. However, for  $Sr_3Ru_2O_7$ ,  $T^*$  is much lower [13]; a first-order transition with very small hysteresis occurs only at temperatures below 1.2 K for  $H \parallel ab$ . Quantum fluctuations occur in  $Sr_3Ru_2O_7$  because its  $T^*$  is close to zero temperature [4–7], while, for  $Sr_4Ru_3O_{10}$ ,  $T^*$  is far above zero temperature, so critical fluctuations near its metamagnetic transition are expected to be weak. From the measurements of  $\rho_{ab}(T)$  in the downward field sweep, we have indeed observed evidence of weak critical fluctuations in  $Sr_4Ru_3O_{10}$ , as shown in Fig. 3(d).

It has been suggested that a new phase occurs in the vicinity of the quantum critical end point of  $Sr_3Ru_2O_7$  [6]. Binz *et al.* recently proposed a theoretical model to interpret the origin of this phase [11]. They generalize the theory of Condon domains [14] to the case of itinerant metamagnets and consider a model for a specific 2D electron system whose Fermi level is close to a van Hove singularity. They find that dipolar magnetostatic forces in an itinerant metamagnet can lead to magnetic domain formation in a finite region of the  $T$ - $H$  phase diagram. Our experimental observations in  $Sr_4Ru_3O_{10}$  seem consistent with this theoretical result, though currently it is not clear if the domains observed here show the spatial distribution we would expect from Condon-like domains [11]. Further experimental inquiries via magneto-optical imag-

ing or scanning SQUID are needed to identify the exact nature of these domains.

Finally, it is worthwhile to point out that steps in magnetoresistivity and magnetization were previously reported in manganites [15,16], where they are associated with an electronic phase separation occurring between an AFM insulating phase and a FM metallic phase. It is known that manganites exhibit an interplay of charge, spin, lattice, and orbital degrees of freedom [17]. The strong coupling of charge carriers to a Jahn-Teller (JT) lattice distortion of  $Mn^{3+}O_6$  results in the formation of polarons. The interaction of orbital degrees of freedom with electron spins and the lattice causes orbital ordering. Both polarons and orbital ordering play important roles in the essential physics of manganites [17]. It is natural to ask if polarons or orbital ordering occurs in  $Sr_4Ru_3O_{10}$ ; although we do not have a definitive answer to this question at present, further investigation of this issue would certainly be very interesting, since  $Ru^{4+}$  is an active JT ion and the structural changes arising from the JT distortion in  $Sr_4Ru_3O_{10}$  have already been observed [8]. Additionally, orbital degrees of freedom have been found to be important in other related ruthenates such as  $Ca_{2-x}Sr_xRuO_4$  [18].

We would like to thank Dr. W. Bao, Dr. B. Binz, Dr. Y. Liu, Dr. Y. Maeno, Dr. M. Norman, Dr. M. Salamon, Dr. P. Schiffer, Dr. M. Sigrist, and Dr. I. Vekhter for useful discussions, and D. Fobes for technical support. This work was supported by the Louisiana Board of Regents support fund LEQSF(2003-06)-RD-A-26 and pilot fund NSF/LEQSF(2005)-Pfund-23, and DARPA Grant No. MDA972-02-1-0012. Z. Q. M. thanks the Research Corporation for financial support.

---

\*Electronic address: zmao@tulane.edu.

- [1] K. Ishida *et al.*, Nature (London) **396**, 658 (1998).
- [2] A. Mackenzie and Y. Maeno, Rev. Mod. Phys. **75**, 657 (2003).
- [3] K.D. Nelson *et al.*, Science **306**, 1151 (2004).
- [4] R. S. Perry *et al.*, Phys. Rev. Lett. **86**, 2661 (2001).
- [5] S. A. Grigera *et al.*, Science **294**, 329 (2001).
- [6] S. A. Grigera *et al.*, Science **306**, 1154 (2004).
- [7] A. G. Green *et al.*, Phys. Rev. Lett. **95**, 086402 (2005).
- [8] M. K. Crawford *et al.*, Phys. Rev. B **65**, 214412 (2002).
- [9] G. Cao *et al.*, Phys. Rev. B **68**, 174409 (2003).
- [10] R. Gupta *et al.*, cond-mat/0508438.
- [11] B. Binz, H. B. Braun, T. M. Rice, and M. Sigrist, cond-mat/0509306.
- [12] M. Zhou *et al.*, Mater. Res. Bull. **40**, 942 (2005).
- [13] S. A. Grigera *et al.*, Phys. Rev. B **67**, 214427 (2003).
- [14] J. H. Condon, Phys. Rev. **145**, 526 (1966).
- [15] R. Mahendiran *et al.*, Phys. Rev. Lett. **89**, 286602 (2002).
- [16] S. Hebert *et al.*, J. Solid State Chem. **165**, 6 (2002).
- [17] M. B. Salamon and M. Jaime, Rev. Mod. Phys. **73**, 583 (2001).
- [18] J. S. Lee *et al.*, Phys. Rev. Lett. **89**, 257402 (2002).